Applied Organometallic Chemistry

Received: 1 April 2011 Revised: 24 June 2011 Accepted: 25 June 2011 Published online in Wiley Online Library: 10 August 2011

(wileyonlinelibrary.com) DOI 10.1002/aoc.1831

Copper(II) complexes of hydroxyflavone derivatives as potential bioactive molecule to combat antioxidants: synthesis, characterization and pharmacological activities

K. Nagashri[a], J. Joseph[a]* and C. Justin Dhanaraj[b]

A variety of novel copper complexes were synthesized and characterized of the formulae [Cu(L^1)(OAc)], [CuL^2(H_2O)], [CuL^3(H_2O)], [CuL^4(OAc)], [CuL^5(H_2O)] [CuL^6], [CuL^7], [CuL^8](OAc) and [CuL^9], where L^1–L^9 represents Schiff base ligands [derived by the condensation of 5-hydroxyflavone with 4-aminoantipyrine (L^1), *o*-aminophenol (L^2), *o*-aminobenzoic acid (L^3), *o*-aminothiazole (L^4), thiosemicarbazide (L^5), 4-aminoantipyrine-*o*-aminophenol (L^6), 4-aminoantipyrine-*o*-aminobenzoic acid (L^7), 4-aminoantipyrine-*o*-aminothiazole(L^8) and 4-aminoantipyrine-thiosemicarbazide (L^9)]. The spectral and magnetic results of the Cu(II) complexes exhibit square planar geometry. The DNA binding properties of copper complexes were studied by using electronic absorption spectra, viscosity and thermal denaturation experiments. The results show that the complexes were interacting with calf thymus (CT DNA). The *in vitro* antimicrobial activities of the investigated compounds were tested against the bacterial species and fungal species. Superoxide dismutase and antioxidant activities of the copper complexes have also been studied.

Keywords: screening; antioxidant; inhibition; superoxide dismutase; thermal denaturation

Introduction

Much research indicates that metal complexes have the ability to bind and nick double-stranded deoxyribonucleic acid (ds-DNA) under physiological conditions.[1–3] In addition, DNA is the primary target molecule for most anticancer and antiviral therapies. Thus, investigations of the interactions of DNA with metal complexes are basic for designing new types of pharmaceutical molecules.[4,5]

The Schiff bases have been the subject of great interest for a number of years because of their various chemical and structural characteristics and also their proved applications as biologically active molecules.[6] Their complexes are known to be biologically important and to act as models to understand the structure of biomolecules and metalloproteins. They also have a variety of applications, including biological, clinical, analytical and also industrial purposes.[7] Interest in the study of Schiff bases and their complexes containing oxygen and nitrogen donor atoms arises from their significant antifungal activity.[8] Inhibition of tumour growth was recently demonstrated for some Schiff base complexes.[9]

Schiff bases of 4-aminoantipyrine and its complexes are known for their variety of applications in the areas of catalysis, clinical applications and pharmacology.[10] Antipyrine and its derivatives possess antibacterial and antitumour activities.[11] New kinds of chemo-therapeutic agents containing Schiff bases have gained significant attention among biochemists and, of those, aminopyrines are commonly administered intravenously to detect liver disease in clinical treatment.[12]

2-Aminothiazoles are a remarkably versatile group of compounds that have found applications in drug development. For instance, these compounds have been used for the treatment of allergies, hypertension, inflammation and for bacterial and HIV infections. Likewise, the unusual antitumour activity of 2-(4-aminophenyl) benzothiazole was originally discovered in a programme of screening for tyrosine kinase inhibitors. Since this discovery, analogues based on the aminothiazole scaffold have been synthesized that display superior growth inhibitory properties. The structures of these compounds show remarkable and intriguing pharmacological properties and their biological profile is unlike that of any known biological agent. Flavones constitute one of the major classes of naturally occurring products. Synthesis of flavones and their derivatives has attracted considerable attention owing to their significant biocidal,[13] pharmaceutical[14] and antioxidant[15] activities. It has been observed that the presence of hydroxyl groups at position 5 or 7 is frequently required for higher biological activities.[16] On the other hand, aminoflavones have been studied as tyrosine kinase inhibitors[17] and as antimitotic agents.[18]

Coordination of organic compounds with metal, i.e. chelation, causes drastic change in the biological properties of the ligand and also the metal moiety. In particular, copper is an important metal and is extensively used for industrial, agricultural and domestic

* *Correspondence to: J. Joseph, Department of Chemistry, Noorul Islam Centre for Higher Education, Kumaracoil-629 180, India. E-mail: chem_joseph@yahoo.co.in*

a *Department of Chemistry, Noorul Islam Centre for Higher Education, Kumaracoil-629 180, India*

b *Department of Chemistry, Anna University Tirunelveli, University VOC College of Engineering, Thoothukudi, India*

purposes owing to its properties of high electrical conductivity, chemical stability, plasticity and capacity to form alloys with many metals. Copper is widespread in the environment, where its determination is necessary because it is known to be toxic at higher concentrations and causes dyslexia, hypoglycemia, gastrointestinal problems and Wilson's disease.[19,20] Cu(II) is also involved in the causation and cure of cancer.[21]

To design improved drugs that target the cellular DNA and to understand the mechanism of action at the molecular level, we therefore decided to examine the synthesis and biological properties of Schiff base copper complexes derived from 4-aminoantipyrine/*o*-aminothiazole and other ligands. Furthermore, we have tested the antimicrobial activity of the synthesized ligands and their complexes using bacteria such as *Staphylococcus aureus, Escherichia coli, Klebsiella pneumaniae, Proteus vulgaris* and *Pseudomonas aeruginosa* and fungi such as *Aspergillus niger, Rhizopus stolonifer, Aspergillus flavus, Rhizoctonia bataicola* and *Candida albicans*. Superoxide dismutase and antioxidant activities of copper complexes have also been measured and compared.

Experimental

Materials and Methods

The chemicals used were of AnalaR grade. Copper(II) acetate was obtained from Merck. Micro analytical data (Carlo Erba 1108, accuracy ±5%) of the compounds were recorded at the Regional Sophisticated Instrumentation Center, Central Drug Research Institute, Lucknow. The amount of copper present in the copper complexes was estimated using ammonium oxalate method. The NMR spectra of the ligands were recorded using Tetramethylsilane (TMS) as internal standard. Chemical shifts (δ) are expressed in units of parts per million relative to TMS. The Fast Atom Bombardment (FAB) mass spectra of the ligands and their complexes were recorded on a Jeol SX 102/DA-6000 mass spectrometer/data system using argon/xenon (6 kV, 10 mA) as the FAB gas. The accelerating voltage was 10 kV and the spectra were recorded at room temperature using *m*-nitrobenzylalcohol (NBA) as the matrix. Molar conductance of the copper complexes was measured in Dimethylsulphoxide (DMSO) solution using a coronation digital conductivity meter. The IR spectra of the ligands and their copper complexes were recorded on a Perkin–Elmer 783 spectrophotometer in 4000–200 cm^{-1} range using a KBr disc. Electronic spectra were recorded with a Systronics 2201 double beam UV–vis spectrophotometer in the 200–1100 nm region. The magnetic susceptibility values were calculated using the relation $\mu_{eff} = 2.83\ (\chi_m.T)^{1/2}$. The diamagnetic corrections were made by Pascal's constant and $Hg[Co(SCN)_4]$ was used as a calibrant. The ESR spectra of the copper complexes were recorded at 300 and 77 K on a Varian E112 X-band spectrometer. Cyclic voltammetric measurements were performed using a glassy carbon working electrode, Pt wire auxiliary electrode and an Ag–AgCl reference electrode. Tetrabutylammoniumperchlorate was used as the supporting electrolyte. All solutions were purged with N_2 for 30 min prior to each set of experiments. The X-ray diffractometer system Jeol JDX 8030 was used to record powder data for the copper complexes, at the Central Elelectrochemical Research Institute, Karaikudi. Solutions of CT DNA in 50 mM NaCl/5 mM Tris–HCl (pH = 7.0) gave a ratio of UV absorbance at 260 and 280 nm, A_{260}/A_{280} of ca. 1.8–1.9, indicating that the DNA was sufficiently free of protein contamination. The DNA concentration was determined by the UV absorbance at 260 nm after 1:100 dilutions. The molar absorption coefficient was taken as 6600 $M^{-1}\ cm^{-1}$. Stock solutions were kept at 4 °C and used after not more than 4 days. CT DNA was purchased from Himedia Chemicals Co. Ltd.

Preparation of Ligands L^1–L^5

5-Hydroxyflavone was synthesized from 2,6-dihydroxyacetophenone according to the method of Looker *et al*.[22] and identified by elemental analysis, melting point, IR and UV spectrum.

Equimolar amounts of 5-hydroxyflavone and 4-aminoantipyrine (L^1), *o*-aminophenol (L^2), *o*-aminobenzoic acid (L^3), *o*-aminothiazole (L^4) and thiosemicarbazide (L^5) were dissolved in ethanol (40 ml). Acetic acid (1.0 ml) was added to this solution. The solution was stirred for 3 h and precipitates formed. The precipitate was filtered and washed with water and ethanol.

L^1

Yield: 76%. Anal. calcd for $C_{26}H_{21}N_3O_3$: C, 73.74; H, 4.99; N, 9.90. Found: C, 73.68; H, 4.91; N, 9.82. FAB mass spectrometry (FAB-MS): *m/z* 424 [M + 1]. ^{1}H-NMR (400 MHz, $CDCl_3$, δ, ppm): 3.0 (1H, s, 3-H), 6.4–7.5 (13H, m, Ar–H), 1.5 (3H, s, H_3C–C), 1.8 (s, 3H, H_3C–N) and 11.2 (1H, s, O–H, D_2O exchangeable). ^{13}C-NMR (400 MHz, $CDCl_3$, ppm): 10.1 (H_3**C**–C), 18.9 (H_3**C**–N), 142.2 (H_3C–**C**), 164.2 (**C**=O), 152.8 (=C–N), 122.5 (C-2), 116.8 (C-3), 153.9 (C-4), 117.7 (C-5), 145.8 (C-6), 122.5 (C-7), 125.8 (C-8), 156.2 (C-9), 120.1 (C-10), 132.5 (C-1′), 126.3 (C-2′, 6′), 140.6 (C-3′, 5′), 132.5 (C-4′), 125.4 (C-1″), 118.2 (C-2″, 6″), 117.5 (C-3″, 5″) and 120.4 (C-4″).

L^2

Yield: 60%. Anal. calcd for $C_{21}H_{15}NO_3$: C, 76.58; H, 4.59; N, 4.25. Found: C, 76.50; H, 4.52; N, 4.18. FAB mass spectrometry (FAB-MS), *m/z* 330 [M + 1]. ^{1}H-NMR (400 MHz, $CDCl_3$) δ: 3.1 (1H, s, 3-H), 6.6–7.8 (12H, m, Ar–H) and 11.2 and 10.8 (2H, s, O–H, D_2O exchangeable, 5-hydroxyflavone and *o*-aminophenol moities). ^{13}C-NMR (400 MHz, $CDCl_3$, ppm): 150.6 (C-2), 102.4 (C-3), 154.6 (C-4), 142.8 (C-5), 144.6 (C-6), 121.4 (C-7), 124.9 (C-8), 154.6 (C-9), 118.8 (C-10), 133.6 (C-1′), 124.3 (C-2′, 6′), 126.5 (C-3′, 5′), 126.4 (C-4′), 130.6 (C-1″), 115.2 (C-2″), 120.6 (C-3″), 119.2 (C-4″), 126.2 (C-5″) and 140.8 (C-6″).

L^3

Yield: 65%. Anal. calcd for $C_{22}H_{15}NO_4$: C, 73.94; H, 4.23; N, 3.91. Found: C, 73.88; H, 4.16; N, 3.88. FAB mass spectrometry (FAB-MS), *m/z* 358 [M + 1]. ^{1}H-NMR (400 MHz, $CDCl_3$) δ: 2.9 (1H, s, 3-H), 6.7–7.9 (12H, m, Ar–H), 11.6 and 10.4 (2H, s, O–H, D_2O exchangeable, 5-hydroxyflavone and *o*-aminobenzoic acid moities). ^{13}C-NMR (400 MHz, $CDCl_3$, ppm): 149.4 (C-2), 110.2 (C-3), 154.5 (C=N), 115.6 (C-5), 146.4 (C-6), 122.8 (C-7), 126.4 (C-8), 152.6 (C-9), 119.9 (C-10), 132.5 (C-1′), 125.4 (C-2′, 6′), 127.6 (C-3′, 5′), 126.5 (C-4′), 148.6 (C-1″), 113.4 (C-2″), 132.6 (C-3″), 116.5 (C-4″), 128.9 (C-5″), 140.8 (C-6″) and 168.2 (COOH).

L^4

Yield: 62%. Anal. calcd for $C_{18}H_{12}N_2O_2S$: C, 67.49; H, 3.78; N, 8.75. Found: C, 67.42; H, 3.72; N, 8.69. Fast atom bombardment mass spectrometry (FAB-MS), *m/z* 322 [M + 1]. ^{1}H-NMR (400 MHz, $CDCl_3$) δ: 2.7 (1H, s, 3-H), 5.1(1H, dd, *J*, 10.5 Hz, -CH=CH-) and 5.4 (1H, dd, *J*, 10.5 Hz, -CH=CH-), 5.9–7.9 (8H, m, Ar–H), 12.9 (1H, s, O–H, D_2O exchangeable). ^{13}C-NMR (400 MHz, $CDCl_3$): 149.4 (C-2), 110.2 (C-3), 154.5 (C=N), 115.6 (C-5), 147.4 (C-6), 122.6 (C-7), 126.9 (C-8), 154.6 (C-9), 121.9 (C-10), 132.5 (C-1′), 125.4 (C-2′, 6′), 127.6 (C-3′, 5′), 126.5 (C-4′), 158.6 (C-11), 103.4 (C-12) and 148.9 (C-13).

L[5]

Yield: 70%. Anal. calcd for $C_{16}H_{13}N_3O_2S$: C, 61.72; H, 4.20; N, 13.49. Found: C, 61.65; H, 4.15; N, 13.40. Fast atom bombardment mass spectrometry (FAB-MS), *m/z* 311 [M + 1]. ^{1}H-NMR (400 MHz, $CDCl_3$) δ: 3.3 (1H, s, 3-H), 6.9–7.8 (8H, m, Ar–H), 11.4 (1H, s, -NH), 8.0 (1H, s, br, HN of -NH_2), 7.5 (1H, s, br, HN of -NH_2), 11.5 (1H, s, O–H, D_2O exchangeable). ^{13}C-NMR (400 MHz, $CDCl_3$): 168.2 (C═O), 149.4 (C-2), 110.2 (C-3), 154.5 (C═N), 115.6 (C-5), 146.9 (C-6), 123.5 (C-7), 124.8 (C-8), 152.6 (C-9), 119.5 (C-10), 132.5 (C-1′), 125.4 (C-2′, 6′), 127.6 (C-3′, 5′), 126.5 (C-4′) and 176.9 (C═ S).

Preparation of Ligands L[6]–L[9]

Equimolar volumes of 5-hydroxyflavone and 4-aminoantipyrine-o-aminophenol (L[6]), *o*-aminobenzoic acid (L[7]), *o*-aminothiazole (L[8]) and thiosemicarbazide (L[9]) were dissolved in ethanol (40 ml). Acetic acid (1.0 ml) was added to this solution. The solution was refluxed for 6 h with stirring and a yellow precipitate formed (Scheme 1). The precipitate was filtered and washed with water and ethanol.

L[6]

Yield: 65%. Anal. calcd for $C_{32}H_{26}N_4O_3$: C, 74.69; H, 5.09; N, 10.88. Found: C, 74.62; H, 5.01; N, 10.82. FAB mass spectrometry (FAB-MS): *m/z* 515 [M + 1]. ^{1}H-NMR (400 MHz, $CDCl_3$, δ, ppm): 2.9 (1H, s, 3-H), 6.6–7.7 (17H, m, Ar–H), 1.4 (3H, s, H_3C–C), 1.7 (3H, s, H_3C–N) and 11.0 and 11.4 (2H, s, O–H, D_2O exchangeable, 5-hydroxyflavone and *o*-aminophenol moieties). ^{13}C-NMR (400 MHz, $CDCl_3$, ppm): 10.1 (H_3**C**–C), 18.9 (H_3**C**–N), 142.1 (H_3C–**C**), 151.6 (═C–N), 154.5 (C═N), 122.3 (C-2), 115.8 (C-3), 153.7 (C-4), 116.7 (C-5), 144.7 (C-6), 122.86 (C-7), 125.8 (C-8), 156.1 (C-9), 118.1 (C-10), 132.4 (C-1′), 127.1 (C-2′, 6′), 140.4 (C-3′, 5′), 132.5 (C-4′), 125.2 (C-1″), 118.0 (C-2″, 6″), 117.3 (C-3″,5″), 120.0 (C-4″), 129.6 (C-1‴), 115.2 (C-2‴), 120.6 (C-3‴), 119.1 (C-4‴), 126.1 (C-5‴) and 139.2 (C-6‴).

L[7]

Yield: 69%. Anal. calcd for $C_{33}H_{26}N_4O_4$: C, 73.04; H, 4.83; N, 10.32. Found: C, 72.95; H, 4.75; N, 10.26. FAB mass spectrometry (FAB-MS), *m/z* 543 [M + 1]. ^{1}H-NMR (400 MHz, $CDCl_3$) δ: 3.1 (1H, s, 3-H), 6.8–7.9 (17H, m, Ar–H), 1.2 (3H, s, H_3C–C), 1.8 (s, 3H, H_3C–N) and 11.2 and 10.9 (2H, s, O–H, D_2O exchangeable, 5-hydroxyflavone and *o*-aminobenzoic acid moities). ^{13}C-NMR (400 MHz, $CDCl_3$, ppm): 10.5 (H_3**C**–C), 18.8 (H_3**C**–N), 142.0 (H_3C–**C**), 153.1 (═C–N), 154.5 (C═N of *o*-aminobenzoic acid moiety), 122.5 (C-2), 116.7 (C-3), 153.8 (C-4), 117.8 (C-5), 145.9 (C-6), 122.4 (C-7), 125.7 (C-8), 156.2 (C-9), 120.2 (C-10), 132.4 (C-1′), 126.2 (C-2′, 6′), 140.5 (C-3′, 5′), 132.5 (C-4′), 125.3 (C-1″), 118.2 (C-2″, 6″), 117.4 (C-3″, 5″), 120.4 (C-4″), 147.2 (C-1‴), 113.4 (C-2‴), 132.5 (C-3‴), 116.6 (C-4‴), 128.8 (C-5‴), 139.4 (C-6‴) and 166.4 (COOH).

L[8]

Yield: 60%. Anal. calcd for $C_{29}H_{23}N_5O_2S$: C, 68.89; H, 4.58; N, 13.85. Found: C, 68.82; H, 4.52; N, 13.78. Fast atom bombardment mass spectrometry (FAB-MS), *m/z* 507 [M + 1]. ^{1}H-NMR (400 MHz, $CDCl_3$) δ: 3.4 (1H, d, *J*, 10.5 Hz, -CH═CH-), 3.6 (1H, d, *J*, 10.5 Hz, -CH═CH-), 6.2–7.9 (13H, m, Ar–H), 1.5 (3H, s, H_3C–C), 2.1 (s, 3H, H_3C–N) and 12.9 (1H, s, O–H, D_2O exchangeable). ^{13}C-NMR (400 MHz, $CDCl_3$, ppm): 10.3 (H_3**C**–C), 19.1 (H_3**C**–N), 142.4 (H_3C–**C**), 151.1 (═C–N), 168.2 (-N═C–N═), 122.8 (C-2), 116.9 (C-3), 153.9 (C═N), 118.1 (C-5), 146.0 (C-6), 123.4 (C-7), 126.6 (C-8), 156.0 (C-9), 120.4 (C-10), 132.6 (C-1′), 126.8 (C-2′, 6′), 140.9 (C-3′, 5′), 132.8 (C-4′), 125.6 (C-1″), 119.1 (C-2″, 6″), 118.2 (C-3″, 5″), 121.5 (C-4″), 157.5 (C-11), 102.2 (C-12) and 148.1 (C-13).

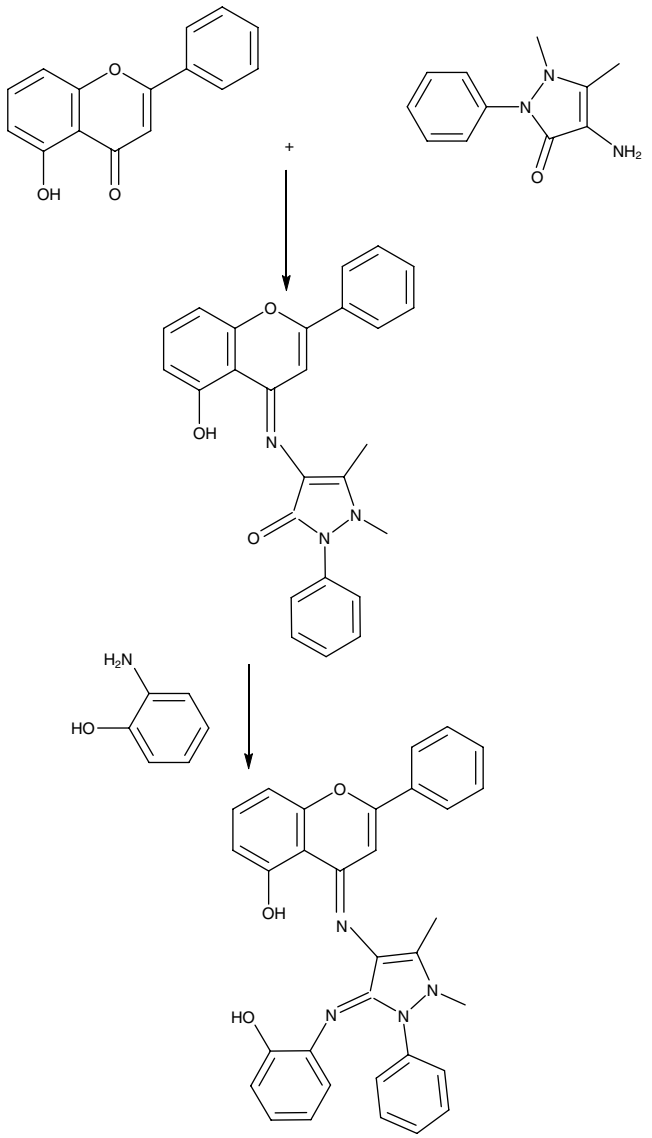

Scheme 1. Synthesis of Schiff base ligand L[1].

L[9]

Yield: 56%. Anal. calcd for $C_{27}H_{24}N_6O_2S$: C, 65.30; H, 4.87; N, 16.92. Found: C, 65.24; H, 4.83; N, 16.86. Fast atom bombardment mass spectrometry (FAB-MS), *m/z* 497 [M + 1]. ^{1}H-NMR (400 MHz, $CDCl_3$, ppm) δ: 3.3 (1H, s, 3-H), 6.3–7.8 (13H, m, Ar–H), 1.1 (s, 3H, H_3C–C), 1.6 (s, 3H, H_3C–N) and 12.2 (1H, s, O–H, D_2O exchangeable), (2H, s, -NH_2). ^{13}C-NMR (400 MHz, $CDCl_3$, ppm): 10.5 (H_3**C**–C), 18.9 (H_3**C**–N), 142.6 (H_3C–**C**), 151.9 (═C–N), 122.9 (C-2), 117.4 (C-3), 154.2 (C-4), 118.1 (C-5), 146.4 (C-6), 122.9 (C-7), 126.2 (C-8), 156.9 (C-9), 120.8 (C-10), 132.9 (C-1′), 127.1 (C-2′, 6′), 141.5 (C-3′, 5′), 133.2 (C-4′), 125.9 (C-1″), 118.8 (C-2″, 6″), 118.4 (C-3″, 5″), 121.6 (C-4″) and 169.9 (C═S). The proposed structures of ligands are given in Fig. 1.

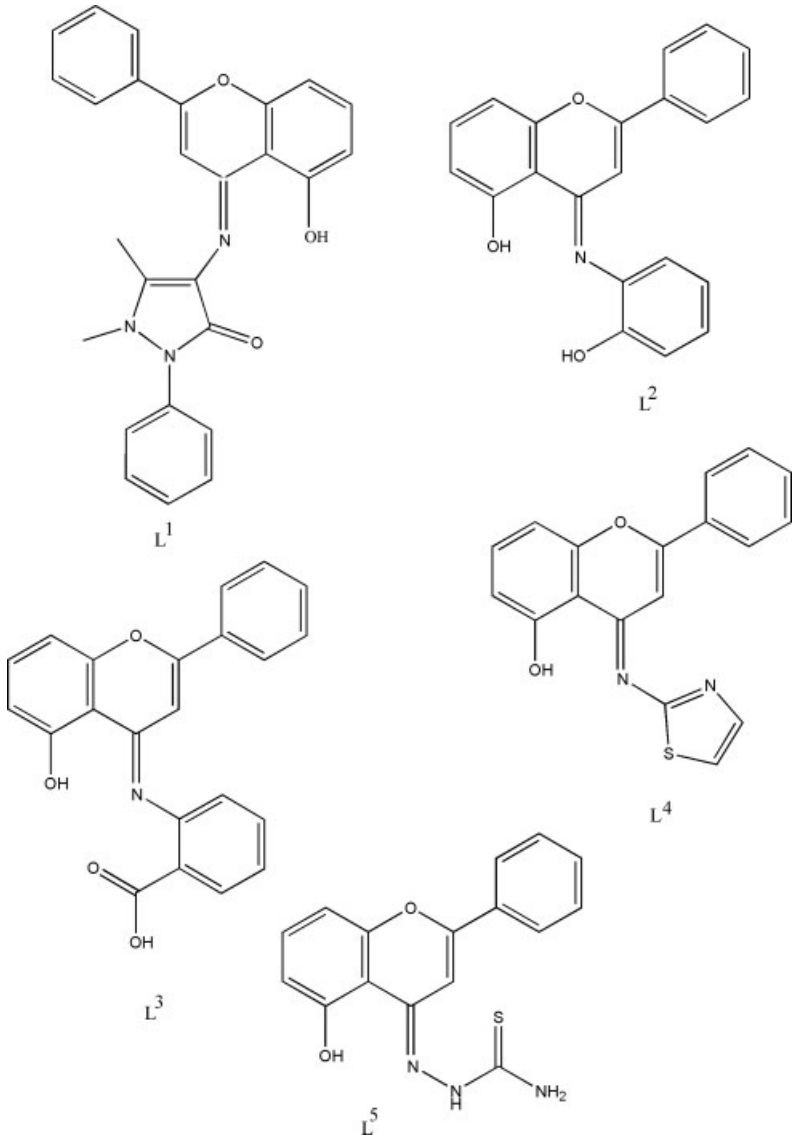

Figure 1. The proposed structures of ligands L^1–L^5.

Preparation of Copper Complexes of Ligands (L^1–L^9)

The ligands (0.05 mM) and copper acetate (0.05 mM) were dissolved in acetone (20 ml). Under stirring, triethylamine (0.075 mM) was then dropped to the mixture with caution. After stirring for 4 h at room temperature, the precipitate was separated by suction filtration, purified by washing several times with acetone and dried in vaccum.

Complex of L^1

Yield: 62%. Anal. calcd for $CuC_{28}H_{24}N_3O_5$: C, 61.57; H, 4.43; N, 7.70, Cu, 11.64. Found: C, 61.52; H, 4.37; N, 7.65; Cu, 11.61. FAB mass spectrometry (FAB-MS), *m/z* 545 [M + 1]. μ_{eff} (BM) = 2.06; Λ_m (mho cm^2 mol^{-1}) = 18.

Complex of L^2

Yield: 74%. Anal. calcd for $CuC_{21}H_{17}NO_4$: C, 61.36; H, 4.17; N, 3.41, Cu, 15.47. Found: C, 61.31; H,4.15; N, 3.36; Cu, 15.43. FAB mass spectrometry (FAB-MS), *m/z* 411 [M + 1]. μ_{eff} (BM) = 1.92; Λ_m (mho cm^2 mol^{-1}) = 24.

Complex of L^3

Yield: 79%. Anal. calcd for $CuC_{22}H_{17}NO_5$: C, 60.18; H, 3.91; N, 3.19, Cu, 14.49. Found: C, 60.14; H, 3.86; N, 3.15; Cu, 14.43. FAB mass spectrometry (FAB-MS), *m/z* [M + 1]. μ_{eff} (BM) = 2.06; Λ_m (mho cm^2 mol^{-1}) = 22.

Complex of L^4

Yield: 76%. Anal. calcd for $CuC_{20}H_{15}N_2O_4S$: C, 54.22; H, 3.42; N, 6.33; Cu, 14.36. Found: C, 74.62; H, 3.35; N, 6.29; Cu, 14.31. FAB mass spectrometry (FAB-MS), *m/z* 443 [M + 1]. μ_{eff} (BM) = 1.98; Λ_m (mho cm^2 mol^{-1}) = 16.

Complex of L^5

Yield: 60%. Anal. calcd for $CuC_{16}H_{15}N_3O_3S$: C, 48.90; H, 3.85; N, 10.70; Cu, 16.18. Found: C, 74.62; H, 3.81; N, 10.63; Cu, 16.14. FAB

mass spectrometry (FAB-MS), *m/z* 393 [M + 1]. μ_{eff} (BM) = 2.06; Λ_m (mho cm^2 mol^{-1}) = 29.

Complex of L[6]

Yield: 66%. Anal. calcd for $CuC_{32}H_{26}N_4O_3$: C, 66.47; H, 4.54; N, 9.69; Cu, 11.00. Found: C, 66.43; H, 4.51; N, 9.64; Cu, 10.93. FAB mass spectrometry (FAB-MS), *m/z* 579 [M + 1]. μ_{eff} (BM) = 1.99; Λ_m (mho cm^2 mol^{-1}) = 14.

Complex of L[7]

Yield: 58%. Anal. calcd for $CuC_{33}H_{26}N_4O_4$: C, 65.37; H, 4.33; N, 9.25; Cu, 10.49. Found: C, 65.32; H, 4.28; N, 9.21; Cu, 10.43. FAB mass spectrometry (FAB-MS), *m/z* 606 [M + 1]. μ_{eff} (BM) = 1.88; Λ_m (mho cm^2 mol^{-1}) = 20.

Complex of L[8]

Yield: 76%. Anal. calcd for $CuC_{31}H_{26}N_5O_4S$: C, 62.74; H, 4.18; N, 10.10; Cu, 11.46. Found: C, 62.70; H, 4.14; N, 10.03; Cu, 11.41. FAB mass spectrometry (FAB-MS), *m/z* 556 [M + 1]. μ_{eff} (BM) = 1.98; Λ_m (mho cm^2 mol^{-1}) = 58.

Complex of L[9]

Yield: 80%. Anal. calcd for $CuC_{27}H_{24}N_6O_2S$: C, 57.89; H, 4.32; N, 15.01; Cu, 11.35. Found: C, 74.62; H, 4.27; N, 14.96; Cu, 11.29. FAB mass spectrometry (FAB-MS), *m/z* 561 [M + 1]. μ_{eff} (BM) = 1.90; Λ_m (mho cm^2 mol^{-1}) = 10. The Schiff base was prepared according to the following scheme (Scheme 1).

Results and Discussion

All the copper complexes are stable at room temperature, insoluble in water but soluble in DMSO and MeCN. The isolated solid complexes of Cu(II) ion with the ligands were subjected to elemental analyses (C, H and N), IR, magnetic moments, molar conductance, ^{1}H NMR and ESR to identify their tentative formulae in a trial to elucidate their molecular structures of copper complexes. Analytical data of the ligands and their complexes served as a basis for the determination of their empirical formula. The synthesized ligands were checked by comparing the TLC with the starting materials, which resulted in a single spot different from the starting materials. All complexes gave satisfactory elemental analyses results (as shown in the Experimental section) within the limits of experimental error. All complexes decomposed above 280 °C, indicating their thermal stability.[23–25]

Molar Conductance

The molar conductance data for the copper complexes measured in DMSO solution for the 0.001 M solutions are given in the Experimental section. The values of complexes, except [CuL^8](OAc), fall in the range of 10–29 Ω^{-1} cm^2 mol^{-1}, which is within the expected range of 1–35 Ω^{-1} cm^2 mol^{-1} for the complexes to behave as nonelectrolytes.[26] Thus, the complexes have a nonelectrolytic nature as evidenced by the involvement of the acetate group in coordination. This result was confirmed from the chemical analysis of the CH_3COO^- ion not precipitated by addition of $FeCl_3$. The [CuL^8](OAc) complex shows a 1:1 electrolytic nature, which was confirmed by the chemical analysis of CH_3COO^- ion precipitated by the addition of $FeCl_3$. This shows that the complex has a 1 : 1 electrolytic nature as evidenced by the noninvolvement of the acetate group in coordination.

IR Spectra

The IR spectra of the ligands show a ν(C=N) peak in the region 1645–1632 cm^{-1}. The IR spectra of all complexes show ν(C=N) bands at 1629–1590 cm^{-1},[27] and the ν(C=N) bands in the complexes are shifted to lower energy regions compared with the free ligands. The shift of this band towards the energy side is probably caused by an increase in the C=N bond order owing to the coordination of the nitrogen with the copper atom.

However, the spectra of complexes show two characteristic bands at 1630–1602 and 1404–1344 cm^{-1}, attributed to υ_{asy}(COO$^-$) and υ_{sy}.(COO$^-$), respectively, indicating the participation of the carboxylate oxygen atom in the complexes. The mode of coordination of carboxylate group has often been deduced from the magnitude of the observed separation between the υ_{asy}(COO$^-$) and υ_{sy}.(COO$^-$). The separation value (*A*) between υ_{asy}(COO$^-$) and υ_{sy}.(COO$^-$) in copper complexes was more than 200 cm^{-1} (260–216 cm^{-1}), suggesting the coordination of carboxylate group in copper complexes of the ligands in a monodentate fashion.[28] The Schiff base ligands display a band around 844 cm^{-1}, ascribed to υ(C–S–C),[29] which shifts to lower frequencies in their spectra of copper complexes in the region 838–832 cm^{-1}, suggesting the coordination of copper ion through the sulfur atom of thioazole moiety. The band at 3466 cm^{-1} for υ(OH) in the free ligand disappeared on complexation, indicating coordination through a deprotonated oxygen.

In the IR spectra of the ligands, two sharp bands at ca. 3436 and 3352 cm^{-1}, probably owing to asymmetric and symmetric vibrations of the NH_2 group, do not undergo any change in the spectra of the complexes, indicating the noninvolvement of the NH_2 group on coordination. In the spectrum of copper complexes, the coordination of azomethine nitrogen atom is further substantiated by the observed positive shift of 34–48 cm^{-1} in the N–N stretching mode in the complexes. Monodentate coordination of the N–N moiety is reported to increase its stretching frequency by this amount. The absence of thioamide band ν(HN–C=S) at ca. 782–813 cm^{-1} and the appearance of new band at ca. 610–631 cm^{-1} confirmed the conversion of ν(C=S) into the ν(C–S) band. The reduction of the thioamide band ν(N=C–SH) observed at ca. 982 cm^{-1} suggests that coordination occurs through the S atom. The IR spectra of complexes show new band owing to the stretching vibrations of > C=N–N=C < bonds at 1568–1560 cm^{-1}.

The band observed in the region 1534–1526 cm^{-1} is due to the $\nu_{C=C}$ stretching of the aromatic ring system. In all the copper–Schiff base complexes, most of the band shifts observed in the wave number region 1142–980 cm^{-1} are in agreement with the structural changes observed in the molecular carbon skeleton after complexation, which cause some changes in (C–C) bond lengths. Conclusive evidence of the bonding is also shown by the observation that new bands in the spectra of all copper complexes appear in the low frequency regions at 550–516, 504–498 and 486–448 cm^{-1}, characteristic of υ(M–O), υ(M–N) and υ(M–S) stretching vibrations, respectively, that are not observed in the spectra of both free ligands.[30] The IR bands at 810–854 and 784–799 cm^{-1}, υ(H_2O) of coordinated water, are an indication of the binding of the water molecule to the copper ion.

Electronic Spectra

The electronic absorption spectra of the Schiff base ligands and their copper complexes in DMSO were recorded at room temperature and the band positions of the absorption maxima;

Table 1. Electronic spectral data of ligands and their copper complexes

Sample no.	Compound	Solvent	Absorption (nm)	Band assignment	Geometry
1	L^1	DMSO	215	INCT	–
			312	INCT	
2	L^2	DMSO	232	INCT	–
			336	INCT	
3	L^3	DMSO	248	INCT	–
			342	INCT	
4	L^1	DMSO	215	INCT	–
			308	INCT	
5	L^2	DMSO	232	INCT	–
			336	INCT	
6	L^3	DMSO	248	INCT	–
			342	INCT	
7	L^1	DMSO	215	INCT	–
			308	INCT	
8	L^2	DMSO	232	INCT	–
			336	INCT	
9	L^3	DMSO	248	INCT	–
			342	INCT	
10	$[CuL^1(OAc)]$	DMSO	228	INCT	
			342	INCT	
			578	$^2B_{1g} \rightarrow {}^2A_{1g}$	Square planar
11	$[CuL^2(H_2O)]$	DMSO	248	INCT	
			342	INCT	
			530	$^2B_{1g} \rightarrow {}^2A_{1g}$	Square planar
12	$[CuL^3(H_2O)]$	DMSO	254	INCT	
			348	INCT	
			572	$^2B_{1g} \rightarrow {}^2A_{1g}$	Square planar
13	$[CuL^4(OAc)]$	DMSO	228	INCT	
			342	INCT	
			544	$^2B_{1g} \rightarrow {}^2A_{1g}$	Square planar
14	$[CuL^5(H_2O)]$	DMSO	248	INCT	
			342	INCT	
			538	$^2B_{1g} \rightarrow {}^2A_{1g}$	Square planar
15	$[CuL^6]$	DMSO	254	INCT	
			348	INCT	
			569	$^2B_{1g} \rightarrow {}^2A_{1g}$	Square planar
16	$[CuL^7]$	DMSO	228	INCT	
			342	INCT	
			556	$^2B_{1g} \rightarrow {}^2A_{1g}$	Square planar
17	$[CuL^8](OAc)$	DMSO	248	INCT	
			342	INCT	
			538	$^2B_{1g} \rightarrow {}^2A_{1g}$	Square planar
18	$[CuL^9]$	DMSO	254	INCT	
			348	INCT	
			562	$^2B_{1g} \rightarrow {}^2A_{1g}$	Square planar

band assignments and the proposed geometry are listed in Table 1. The electronic spectra of the ligands and their complexes were recorded in DMSO as a solvent. The absorption spectrum for L^1 shows bands at 225 and 312 nm. These bands can be attributed to $n-\pi^*$ and $\pi-\pi^*$ transitions within the Schiff base molecule. The electronic spectrum of the corresponding $[CuL^1(OAc)]$ complex in DMSO reveals a broad band at 558 nm assignable to $^2B_{1g} \rightarrow {}^2A_{1g}$ transition,[31,32] which is characteristic of square planar environment around the copper(II) ion. Similar spectral features were assigned for other complexes.

The electronic spectra of all the complexes exhibit bands in the regions 200–225, 272–332 and 362–390 nm, which may be due to the $\pi-\pi^*$ transition of the benzenoid/or $n-\pi^*$ (COO^-), $\pi-\pi^*$ transition of the > C═N- chromophore and $n-\pi^*$ transition of the > C═N- chromophore, coupled with the secondary band of the benzene ring, respectively. Further, there were a few sharp bands observed in the region 233–257 nm in the spectra of the complexes, which could be assigned as charge transfer bands.

The magnetic susceptibility measurements in the solid state show that the copper complexes were paramagnetic in nature at room temperature. The observed magnetic moments of these

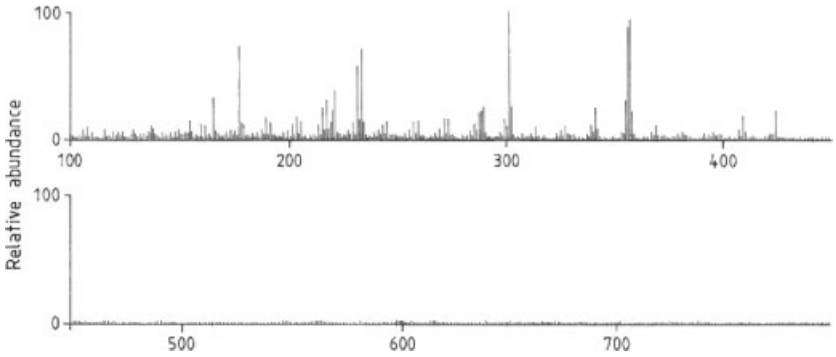

Figure 2. FAB mass spectrum of ligand L^1.

complexes are quite close to the values expected for copper(II) complexes without any metal–metal interaction. The magnetic susceptibility study of the [CuL^1(OAc)] complex gives a magnetic moment value (μ_{eff}) of 2.06 BM at room temperature,[33] which is normal for mononuclear complexes of magnetically diluted d^9 systems with $S = 1/2$ spin state having square planar structure, and there is no metal–metal interaction along the axial position in the complex. A similar magnetic behaviour was observed for other copper complexes.

^{1}H-NMR Spectra

The ^{1}H and ^{13}C-NMR spectra of ligands were recorded in $CDCl_3$ and are given in the Experimental section. All the protons were found to be in their expected region.[34] The conclusions drawn from these studies lend further support to the mode of bonding discussed in their IR spectra. The number of protons calculated from the integration curves and those obtained from the values of the expected CHN analyses agree with each other.

FAB Mass Spectra

Mass spectra provide a vital clue for elucidating the structure of compounds. The mass spectra of the ligand (L^1) and its copper complex [CuL^1(OAc)] were recorded and their stoichiometric compositions were compared, as shown in Figs 1 and 2. The intensity of these peaks reflects the stability and abundance of the ions.[35] The molecular ion peak for the ligand (L^1) is observed at 424 *m/z*, whereas its copper complex shows a molecular ion peak at 515 *m/z*, which confirms the stoichiometry of the copper complexes to be [CuL^1(OAc)] type. Elemental analysis values are in close agreement with the values calculated from molecular formulae assigned to these complexes, which is further supported by the FAB-mass studies of respective complexes. Similar mass spectral features were assigned for other ligands and their copper complexes.

ESR Spectra

The ESR spectrum of the [CuL^1(OAc)] complex was recorded in DMSO at 300 and 77 K. The spectrum at 300 K shows one intense absorption band at high field, which is isotropic owing to the tumbling motion of the molecules. However, this complex in the frozen state shows four well-resolved peaks with low intensities in the low-field region and one intense peak in the high-field region. The magnetic susceptibility value reveals that the copper complex has a magnetic moment of 2.06 BM corresponding to one unpaired electron, indicating that the complex is mononuclear in nature. This fact was also evident from the absence of the half-field signal, observed in the spectrum at 1600 G owing to the $m_s = \pm 2$ transitions, ruling out any Cu–Cu interaction.[36] The ESR spectral data are given in Table 2.

The value of $g_{||} < 2.3$ in the present complex gives a clear indication of the covalent character of the metal–ligand bond and delocalization of the unpaired electron into the ligand. The trend of $g_{||}$ (2.25) > $g_\perp$ (2.04) > g_e (2.0036) describes the axial symmetry with the unpaired electron residing in the $d_{x^2-y^2}$ orbital. For the present Cu(II) complex, the observed *g* values are $g_{||}$ (2.25) > $g_\perp$ (2.04) > g_e (2.0036), which suggest that the unpaired electron lies in the $d_{x^2-y^2}$ orbital. The $A_{||}$ and $A_\perp$ values in the order: $A_{||}$ (155) > $A_\perp$ (38.5) also indicate that the complex has square planar geometry and the system is axially symmetric.[37]

The $g_{||}$ and $A_{||}$ values for square planar CuN_4 chromophore are around 2.2 and 200 cm^{-1} respectively. On replacing the nitrogen donors by oxygen donors, the $g_{||}$ value increases and the $A_{||}$ value decreases and thus the $g_{||}$ and $A_{||}$ values for a CuO_4 chromophore are around 2.42 and 145 cm^{-1}, respectively. Several CuN_2O_2 chromophores have been shown to possess $g_{||}$ and $A_{||}$ values around 2.25 and 160 cm^{-1}. Thus, all the present complexes exhibit $g_{||}$ (2.24–2.26) and $A_{||}$ (148–158) values consistent with a CuN_2O_2 chromophore.

From above EPR data, the *f* values for copper complexes were determined to be in the range of 142–158 cm.[38] Therefore, our synthesized copper complexes exhibiting appreciable square planar distortion are expected to show high superoxide dismutase (SOD)-like activity.

Molecular orbital coefficients α^2 (in-plane σ-bonding), β^2 (in-plane π-bonding) and γ^2 (out-plane π-bonding) were calculated using eqns (1)–(3).

$$\alpha^2 = -(A_{||}/0.036) + (g_{||} - 2.0036) + 3/7\,(g_\perp - 2.0036) + 0.04 \quad (1)$$

$$\beta^2 = (g_{||} - 2.0036)E/ - 8\lambda\alpha^2 \quad (2)$$

$$\gamma^2 = (g_\perp - 2.0036)E/ - 2\lambda\alpha^2 \quad (3)$$

The α^2 value of 0.5 indicates complete covalent bonding, while that of 1.0 suggests complete ionic bonding. The observed value of 0.73 for the present complex indicates that the copper complex has some covalent character. The observed β^2 and γ^2 values of 1.24 and 0.74 indicate that there is interaction in the out-of-plane π-bonding, whereas the in-plane π-bonding is predominantly ionic. Significant information about the nature of bonding in the Cu(II) complex can be derived from the relative magnitudes of $K_{||}$

Table 2. ESR spectral data of the copper complexes

Complex	$g_{\|\|}$	$g_{\perp}$	g_{iso}	$A_{\|\|}$	$A_{\perp}$	$K_{\|\|}$	$K_{\perp}$	α^2	β^2	γ^2	$f(g_{\|\|}/A_{\|\|})$
[CuL^1(OAc)] at 300 K			2.05								
[CuL^1(OAc)] at 77 K	2.25	2.04	–	155	39	0.92	0.54	0.73	1.2	0.74	145
[CuL^2(H_2O)] at 300 K			2.10								
[CuL^2(H_2O)] at 77 K	2.24	2.06	–	148	44	0.86	0.43	0.76	1.4	0.70	151
[CuL^3(H_2O)] at 300 K			2.12								
[CuL^3(H_2O)] at 77 K	2.26	2.05	–	158	52	0.74	0.49	0.81	1.3	0.82	143
[CuL^4(OAc)] at 300 K			2.12								
[CuL^4(OAc)] at 77 K	2.26	2.05	–	158	52	0.74	0.49	0.81	1.3	0.82	143
[CuL^5(H_2O)] at 300 K			2.12								
[CuL^5(H_2O)] at 77 K	2.26	2.05	–	158	52	0.74	0.49	0.81	1.3	0.82	143
[CuL^6] at 300 K			2.12								
[CuL^6] at 77 K	2.26	2.05	–	158	52	0.74	0.49	0.81	1.3	0.82	143
[CuL^7] at 300 K			2.12								
[CuL^7] at 77 K	2.26	2.05	–	158	52	0.74	0.49	0.81	1.3	0.82	143
[CuL^8](OAc) at 300 K			2.12								
[CuL^8](OAc) at 77 K	2.26	2.05	–	158	52	0.74	0.49	0.81	1.3	0.82	143
[CuL^9] at 300 K			2.12								
[CuL^9] at 77 K	2.26	2.05	–	158	52	0.74	0.49	0.81	1.3	0.82	143

Table 3. Cyclic voltammetric data of copper complexes

Complex	E_{pa}	E_{pc}	ΔE_p	Potential assignment
[CuL^1(OAc)]	−0.658	−0.766	108	Cu(II)/Cu(I)
	0.432	–	–	Cu(II)/Cu(III)
[CuL^2(H_2O)]	−0.588	−0.742	154	Cu(II)/Cu(I)
	1.10	–		Ligand oxidation
[CuL^3(H_2O)]	−0.628	−0.768	140	Cu(II)/Cu(I)
	0.464	–	–	Cu(II)/Cu(III)
[CuL^4(OAc)]	−0.600	−0.766	166	Cu(II)/Cu(I)
	0.432	−0.98	–	Cu(I)/Cu(0)
[CuL^5(H_2O)]	−0.650	−0.762	112	Cu(II)/Cu(I)
	0.432	−0.92		Cu(I)/Cu(0)
[CuL^6]	−0.632	−0.742	110	Cu(II)/Cu(I)
	0.364	–	–	Cu(II)/Cu(III)
[CuL^7]	−0.532	−0.702	170	Cu(II)/Cu(I)
	0.282	–	–	Cu(II)/Cu(III)
[CuL^8](OAc)	−0.526	−0.686	160	Cu(II)/Cu(I)
	0.486	–	–	Cu(II)/Cu(III)
[CuL^9]	−0.582	−0.658	132	Cu(II)/Cu(I)
	−1.20	–	–	Ligand oxidation

and $K_{\perp}$.

$$K_{||} = \alpha^2\beta^2 \quad (4)$$

$$K_{\perp} = \alpha^2\gamma^2 \quad (5)$$

For the present complex, the observed order $K_{||}$ (0.92) > $K_{\perp}$ (0.54) implies a greater contribution from out-of-plane π-bonding than from in-plane π-bonding in metal–ligand π-bonding.

Cyclic Voltammetry

The electrochemical behaviour of the Schiff base Cu(II) complexes in DMSO (0.1 M of tetrabutylammoniumperchlorate as supporting electrolyte (scan rate 100 mV s^{-1}) at 300 K in the potential range of +0.8 to −0.8 V) was examined. Table 3 summarizes the potentials and their assignments, which mainly depend on the geometry and environment around the copper ion (i.e. ligand core). The electrochemical data are given in Table 3. Reduction at negative potential is the usual trend observed for phenoxo copper complexes because of the electronegativity and hard nature of the phenoxide atoms in the ligand. The cyclic voltammogram of [CuL^1(OAc)] complex in DMSO solution at 300 K in the potential range +0.6 to −0.8 V at scan rate 0.1 V s^{-1} was recorded. It shows a well-defined redox process corresponding to the formation of the quasi-reversible Cu(II)/Cu(I) couple. The anodic peak at E_{pa} = −0.658 mV vs Ag–AgCl and the associated cathodic peak at E_{pc} = −0.766 mV correspond to the Cu(II)/Cu(I) couple. The [CuL^1(OAc)] complex exhibits a quasi-reversible behaviour. It also shows one irreversible peak at 0.432 mV which was assigned to Cu(II)/Cu(III). Similar electrochemical behaviour was observed and assigned for other complexes.

On comparing the cyclic voltammograms, we observed that the variation in oxidation and reduction potential may be due to distortion in the geometry of the complexes, which arises owing to different donor atoms coordinated to the copper ion. It is concluded that the present ligand systems stabilize the unusual oxidation states of copper ion during electrolysis. It is essential for pharmacological activities and plays a crucial role in curing or prevention of untreatable diseases.

Antimicrobial Activity

The compounds synthesized were evaluated for their antibacterial, antifungal, DNA binding and antioxidant studies. The antibacterial and antifungal tests were carried out using the serial dilution method.

The *in vitro* antimicrobial activities of the investigated compounds were tested against the bacterial species *Staphylococcus aureus, Escherichia coli, Klebsiella pneumaniae, Proteus vulgaris* and *Pseudomonas aeruginosa* and fungal species *Aspergillus niger, Rhizopus stolonifer, Aspergillus flavus, Rhizoctonia bataicola* and

Table 4. Minimum inhibitory of concentration of the synthesized compounds against growth of bacteria (μg ml^{-1})

Sample no.	Compound	*Escherichia coli*	*Klebsiella pneumoniae*	*Proteus vulgaris*	*Pseudomonas aeruginosa*	*Staphylococcus aureus*
1	L^1	60	64	66	66	72
2	L^2	24	26	20	16	28
3	L^3	28	36	26	32	30
4	L^4	60	64	66	66	72
5	L^5	24	26	20	16	28
6	L^6	28	36	26	32	30
7	L^7	60	64	66	66	72
8	L^8	24	26	20	16	28
9	L^9	28	36	26	32	30
10	$[CuL^1(OAc)]$	34	38	32	28	42
11	$[CuL^2(H_2O)]$	26	28	30	26	48
12	$[CuL^3(H_2O)]$	52	54	58	60	63
13	$[CuL^4(OAc)]$	34	38	32	28	42
14	$[CuL^5(H_2O)]$	26	28	30	26	48
15	$[CuL^6]$	52	54	58	60	63
16	$[CuL^7]$	34	38	32	28	42
17	$[CuL^8](OAc)$	26	28	30	26	48
18	$[CuL^9]$	52	54	58	60	63
19	PenicillinG	10	15	6	12	4
20	Ampicillin	12	10	08	04	06
21	Vancomycin	06	14	12	10	08
22	Ofloxacin	08	10	04	06	14

Candida albicans. The minimum inhibitory concentration (MIC) values of the compounds are summarized in Tables 4 and 5. A comparative study of the ligands and their complexes (MIC values) indicates that complexes exhibit higher antimicrobial activity than the free ligands. In this study, the antimicrobial activity of the ligands may be due to the heteroaromatic residues. Compounds containing > C═N group have enhanced antimicrobial activity than > C═C < group. The growth of certain microorganisms takes place even in the absence of O_2. Hence, compounds containing > C═C < group though capable of absorbing O_2 are not related with the growth of microorganisms.

The enhanced activity of the complexes can be explained on the basis of Overtone's concept[39] and Tweedy's chelation theory.[40] According to Overtone's concept of cell permeability, the lipid membrane that surrounds the cell favours the passage of only the lipid-soluble materials, which makes liposolubility an important factor that controls the antimicrobial activity. On chelation, the polarity of the metal ion will be reduced to a greater extent owing to the overlap of the ligand orbital and partial sharing of the positive charge of the metal ion with donor groups. Further, it increases the delocalization of π-electrons over the whole chelate ring and enhances the lipophilicity of the complexes. This increased lipophilicity enhances the permeation of the complexes into lipid membranes and blocking of the metal binding sites in the enzymes of microorganisms. These complexes also disturb the respiration process of the cell and thus block the synthesis of the proteins, which restricts further growth of the organism and as a result microorganisms die.

The increased activity of the complexes can also be explained on the basis of their high solubility, fitness of the particles, size of the metal ion and the presence of the bulkier organic moieties. Formation of a hydrogen bond through the azomethine group with the active centre of cell constituents resultd in interference with the normal cell process.[41] Another mechanism of toxicity of these complexes to microorganisms may be due to the inhibition of energy production or ATP production,[42] by inhibiting respiration or by the uncoupling of oxidative phosphorylation. The biological activity involves inhibition of DNA synthesis[43] by creating lesions in DNA strands by oxidative rupture and by binding the nitrogen bases or DNA or RNA, hindering or blocking base replication. The inhibition growth may be due to the effect on the biosynthesis of phospholipids in cell membrane and proteins.

The observed variation in the activity of the copper complexes across the various classes of organisms studied may be attributable to differences in cell wall and/or membrane construction (Gram-positive bacteria, peptidoglycan and teichoic acid; Gram-negative bacteria, peptidoglycan and liposaccharide). It is expected that the more extensive heteroaromatic ring system of antipyrinyl and the presence of the lipophilic group C═N would confer greater lipophilicity on the copper complexes and enable it to penetrate the cell wall and promote adverse intracellular interactions.

Among the studied compounds, $[CuL^1(OAc)]$ (MIC 6 μg ml^{-1}) complex presented good activity against *Candida albicans*. Since this fungi is very harmful to humans, we consider this result of major importance. This confirms that antibacterial and antifungal activities are dependent on the molecular structure of the ligands and the type of the complex formed. It appears from the above results that Cu(II) Schiff-base complex may be able to maintain good antibacterial and antifungal activities and be an effective antibacterial broad-spectrum drug that may be able to solve some problems of antibacterial resistance.

Interaction of Copper Complexes with Microorganisms

Copper complexes having more biological activitys due to redox processes could be involved in the observed biological activity.

Table 5. Minimum inhibition of concentration of the synthesized compounds against growth of fungi (μg ml^{-1})

Sample no.	Compound	*Aspergillus niger*	*Rhizopus stolonifer*	*Aspergillus flavus*	*Rhizoctonia bataicola*	*Candida albicans*
1	L^1	60	66	72	80	50
2	L^2	72	84	63	77	65
3	L^3	85	76	69	64	102
4	L^4	69	79	88	82	86
5	L^5	88	90	96	70	78
6	L^6	94	102	110	64	94
7	L^7	70	81	70	60	99
8	L^8	84	72	66	56	76
9	L^9	78	65	76	90	80
10	$[CuL^1(OAc)]$	28	30	34	38	32
11	$[CuL^2(H_2O)]$	32	26	46	36	38
12	$[CuL^3(H_2O)]$	52	55	68	80	50
13	$[CuL^4(OAc)]$	28	30	34	38	32
14	$[CuL^5(H_2O)]$	32	26	46	36	38
15	$[CuL^6]$	52	55	68	80	50
16	$[CuL^7]$	28	30	34	38	32
17	$[CuL^8](OAc)$	32	26	46	36	38
18	$[CuL^9]$	52	55	68	80	50
19	Nystatin	10	16	8	14	12
20	Ketoconazole	12	08	16	06	12
21	Clotrimazole	08	06	12	10	04
22	Bavstatin	14	10	08	06	12

$[CuL^1(OAc)]$ in DMSO was mixed into the culture media with different microorganisms (1 mM as final concentration) and their UV–vis spectra were recorded at different times of incubation. Most of the obtained spectra did not have the best quality owing to interference of some of the components of the culture media. The band of $[CuL^1(OAc)]$ in culture media at about 410 nm disappeared after interacting with the different microorganisms. In the case of *Proteus vulgaris* and *Pseudomonas aeruginosa*, against which $[CuL^1(OAc)]$ was active, this band was still observed at 180 min of incubation but completely disappeared after 24 h. It is important to point out that $[CuL^1(OAc)]$ presents a band at 332 nm, indicating that the first transformation of the complex occurred immediately (shift to 410 nm) with a second change at 24 h. The disappearance of the characteristic band of a Cu(I) complex at 332 nm indicates that a redox process took place.

From this observation, each organism takes a different incubation time. During that period, a compound interacts with microorganisms (turbidity was observed) and some redox change occurs [the complex interacts with the microorganism; the electronic absorption band is shifted to a lower wavelength and completely disappears after 24 h (bacteria) and 48 h (fungi)]. The activity may also be due to the compounds containing lipophilic groups (azomethine linkage or heteroaromatic nucleus) crossing the cell membrane of the microorganism and interfering with their processes, causing growth to be inhibited.

Electron Transfer as a Possible Mode of Action

In the present study, the observed cyclic voltammetric behaviour of copper complexes showed that the redox cycle may also be contribute to their inherent toxicity. For example, redox cycling between Cu(II) and Cu(I) can catalyse the production of highly reactive hydroxyl radicals, which can subsequently damage lipids, proteins, DNA and other biomolecules. Further, the potential reduction of the Cu(II)/Cu(I) process is related to the potential SOD mimetic activity. The synthesized copper complexes also have reduction potentials greater than −0.6 V, so it is possible for electron uptake to occur in the biological milieu, followed by donation to an acceptor.

Table 6. Superoxide dismutase activity of some copper(II) complexes

Sample no.	Complex	IC_{50} (mol dm^{-1})
1	$[CuL^1(OAc)]$	86
2	$[CuL^2(H_2O)]$	98
3	$[CuL^3(H_2O)]$	90
4	$[CuL^4(OAc)]$	74
5	$[CuL^5(H_2O)]$	65
6	$[CuL^6]$	72
7	$[CuL^7]$	84
8	$[CuL^8](OAc)$	70
9	$[CuL^9]$	69

SOD Activity

The SOD mimetic activities of the copper(II) complexes were determined and have been compiled in Table 6. In the present complexes, the higher SOD activity was $[CuL^7]$ owing to the presence of electron-withdrawing substituents compared with other complexes. A greater interaction between superoxide ion and Cu(II) complex was induced owing to the stronger axial bond, resulting in an increased catalytic activity. In addition, the designed ligands containing electron-withdrawing substitutent stabilized the Cu(I) complex formed during superoxide dismutation reaction,

which further reacted with superoxide ion to give hydrogen peroxide. The distorted geometry of these complexes may favour the geometrical change, which is essential for catalysis as the geometry of copper in the SOD enzyme also changes from distorted square planar geometry. The difference in reactivities of the synthesized complexes may be attributed to the coordination environment and the redox potential of the couple Cu^{+}/Cu^{2+} in copper(II) complexes during the catalytic cycle. It has been reported that the redox potential of copper (II) ions is affected by the coordination structure of copper(II) complexes. The nature of substituent plays a key role in stabilizing the Cu^{+} oxidation state during the catalytic cycle.[44,45]

Table 7. DNA binding constant and melting temperature data

Complex	K_b (M^{-1})	T_m (°C)	σ_T (°C)
[CuL^1(Oac)]	1.2×10^6	60	26
[$CuL^2(H_2O)$]	2.4×10^6	58	30
[$CuL^3(H_2O)$]	1.8×10^6	69	29
[CuL^4(OAc)]	2.5×10^5	64	25
[$CuL^5(H_2O)$]	3.6×10^5	66	23
[CuL^6]	1.2×10^5	72	31
[CuL^7]	4.2×10^5	66	24
[CuL^8](OAc)	1.4×10^6	62	20
[CuL^9]	2.1×10^6	56	18

DNA Binding Studies

DNA binding studies are important for the rational design and construction of new and more efficient drugs targeted to DNA.[46–48] A variety of small molecules interact reversibly with double-stranded DNA, primarily through three modes: (i) electrostatic interactions with the negative charged nucleic sugar–phosphate structure, which are along the external DNA double helix and do not possess selectivity; (ii) binding interactions with two grooves of the DNA double helix; and (iii) intercalation between the stacked base pairs of native DNA. To explore the mode of the Cu(II) complex binding to DNA, the following experiments were carried out.

Electronic absorption spectroscopy

Electronic absorption spectroscopy is universally employed to determine the binding characteristics of metal complexes with DNA. The intercalative mode of binding usually results in hypochromism and red shift owing to the strong stacking interaction between an aromatic chromophore and the base pairs of DNA. The extent of red shift and hypochromism is commonly found to correlate with the binding strength, but metal complexes that bind nonintercalatively or electrostatically with DNA may result in hyperchromism or hypochromism.[49] Hyperchromic effect and hypochromic effect are the spectral features of DNA concerning its double-helix structure.[50] This spectral change process reflects the corresponding changes of DNA in its conformation and structures after the drug has bound to DNA. Hypochromism results from the contraction of DNA in the helix axis, as well as from the change in conformation on DNA, while hyperchromism results from damage to the DNA double helix structure.

The absorption spectra of the four complexes in the absence and presence of DNA are shown in Fig. 3. In the UV region, the Cu(II) complex exhibits two absorption bands: one at ca. 354 nm and another at ca. 297 nm. With increasing DNA concentration, the absorption bands of the complexes were affected, resulting in a tendency to hypochromism and slight shifts to longer wavelengths, which indicates that the Cu(II) complex can interact with DNA. The observed hypochromism and bathochromism for the Cu(II) complex are large compared with those observed for potential intercalators. The intrinsic binding constant (K_b) was obtained by monitoring the change in absorbance with increasing concentrations of DNA for the Cu(II) complexes (Table 7).

The finding of hypochromism and bathochromism through spectroscopic titration for metal complexes with planar ligands has been previously taken as evidence of intercalation,[51] but such data alone are certainly insufficient to rule out alternative mechanisms. Thus it becomes necessary to carry out hydrodynamic measurements such as viscosity. Such experiments have frequently been used to evaluate structural changes in the DNA helix by intercalative interaction.[52] This increase in the viscosity can be therefore be attributed to the enlargement of the separation between the base pairs, which are pushed apart to accommodate the intercalating molecule.

Viscosity measurements

Hydrodynamic methods, such as determination of viscosity, which is exquisitely sensitive to the change of length of DNA, may be the most effective means studying the binding mode of complexes to DNA in the absence of X-ray crystallographic or NMR structural data.[53] To further confirm the interaction mode of the Cu(II)

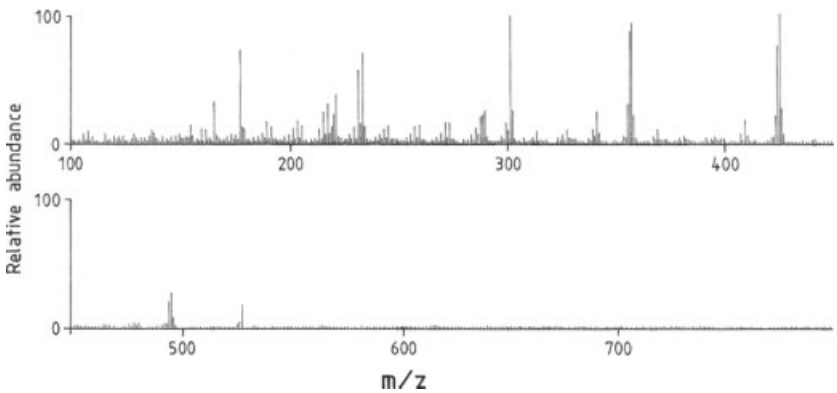

Figure 3. FAB mass spectrum of [$CuL^1(OAc)_2$] complex.

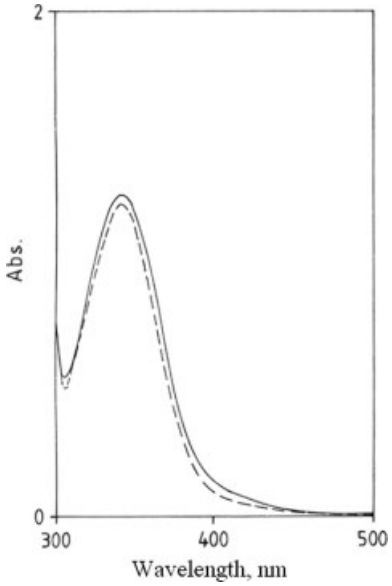

Figure 4. UV–vis, spectra of copper complex in the absence and in the presence of DNA.

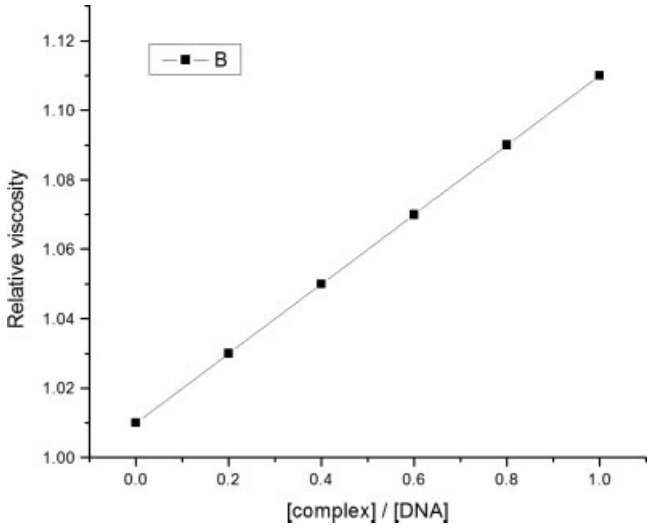

Figure 5. Plot of relative viscosity versus [complex]/[DNA] effect of copper complex on the viscosity of CT DNA at 25 ± 0.1 °C. Copper complex = 0–100 μM. [DNA] = 50 μM.

complex with DNA, a viscosity study was carried out (Fig. 4). The viscosity measurement is based on the flow rate of a DNA solution through a capillary viscometer. The specific viscosity contribution (g) owing to the DNA in the presence of a binding agent was obtained. The results indicate that the absence and presence of the metal complex have a marked effect on the viscosity of the DNA. The specific viscosity of the DNA sample increases obviously with the addition of the complex. The viscosity studies provide a strong argument for intercalation. The viscosity increase of DNA is ascribed to the intercalative binding mode of the drug because this could cause the effective length of the DNA to increase.[54] In essence, the length of the linear piece of B-form DNA is given by the thickness of the base pairs that are stacked along the helix axis in Van der Waals contact with each other. Introducing another aromatic molecule into the stack therefore increases the length. Therefore, the viscosity increase of the DNA caused by the addition of the complex can provide further support for the intercalative mode of the Cu(II) complex.

Thermal denaturation studies

DNA thermal melting is a measure of the stability of the DNA double helix with temperature; an increase in the thermal melting temperature (T_m) indicates an interaction between DNA and the metal complex. In the present case, thermal melting studies were carried out at DNA to complex concentration ratios of 25 and T_m and σT (the temperature range between which 10 and 90% of the absorption increase occurred) values were determined by monitoring the absorbance of DNA at 260 nm as a function of temperature. As shown in Fig. 5, the T_m of DNA in the absence of any added drug was found to be 60 ± 1 °C, under our experimental conditions. Under the same set of conditions, the presence of complexes increased the T_m by 4 and 2 °C, respectively, and the values are given in Table 7.

Hydroxyl radial scavenging activity

The hydroxyl radicals (OH•) in aqueous media were generated through the Fenton system. The hydroxyl radical bleached the

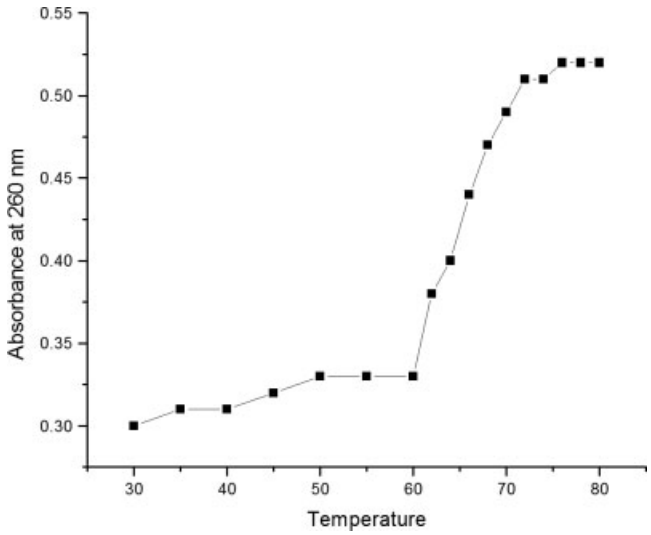

Figure 6. Melting curves of CT DNA in the absence and presence of copper complex.

safranin, and so decreased the absorbance of the reaction mixture, indicating a decrease in hydroxyl radical scavenging ability. The scavenging ratio for $OH^{\cdot}$ was calculated from the following expression:

$$\text{Scavenging ratio (\%)} = [(A_i - A_o)/(A_c - A_o)] \times 100 \qquad (6)$$

where A_i is the absorbance in the presence of the tested compound; A_o is the absorbance of the tested compound; and A_c is the absorbance in the absence of the tested compound, EDTA-Fe(II) and H_2O_2.

Figure 6 depicts the inhibitory effect of the complexes on OH•. The inhibitory effect of the complexes is marked and the suppression ratio increases with increasing concentration in the range of tested concentration. The order of the suppression ratio

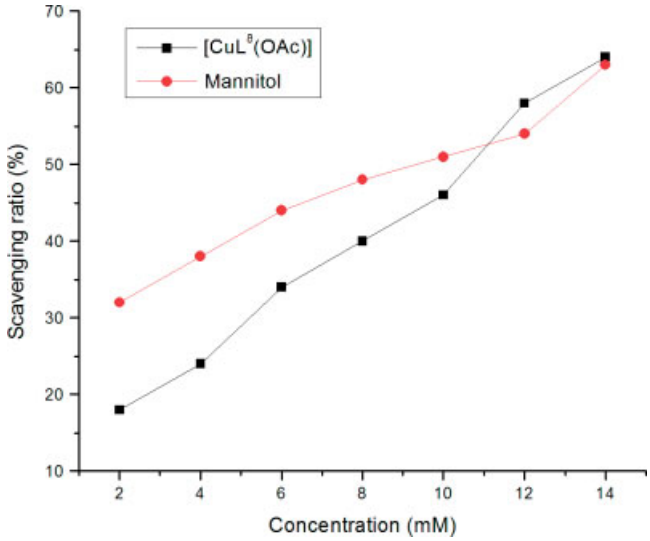

Figure 7. Scavenging effect of copper complexes and mannitol on hydroxyl radicals. Experiments were performed in triplicate.

for OH• is

$$[CuL^9] > [Cu(L^8)(OAc)] > [CuL^7] > [CuL^6] > Cu(L^1)(OAc)] > [CuL^5] > [CuL^4(OAc)] > [CuL^3(H_2O)] > [CuL^2(H_2O)]$$

at different concentrations.

Moreover, mannitol is a well-known natural antioxidant, so we also studied the scavenging activity of mannitol against hydroxyl radical using the same model. As shown in Fig. 7, the 50% inhibitory concentration (IC_{50}) value of mannitol is 9.6 mM. However, the [CuL^2] complex had a similar suppression ratio, and the concentration was higher than that of mannitol. The marked antioxidant activity of complex **1**, in comparison to free ligands, could be due to the coordination of metal in the 4 and 5 positions of the condensed ring system, increasing its capacity to stabilize unpaired electrons and, thereby, to scavenge free radicals.

Conclusion

The new Schiff base ligands and their copper complexes have been synthesized and characterized. The DNA binding properties of copper complexes were studied using absorption spectra, viscosity and thermal denaturation experiments. The results show that the complexes interactied with CT DNA. We also carried out the DNA cleavage using gel electrophoresis techniques. From the antimicrobial study, the presence of lipophilic and polar substituents such as C═N, S–H and NH_2 is expected to enhance the fungal and bacterial toxicity and therefore copper(II) complexes have a greater chance of interaction with the nucleotide bases. It has also been observed that some moieties such as azomethine linkage or heteroaromatic nucleus introduced into such compounds exhibit extensive biological activities that may be responsible for the increase in hydrophobic character and liposolubility of the molecules in crossing the cell membrane of the microorganism and enhanced biological utilization ratio and activity of complexes. The present work has thus shown that copper complexes of Schiff base derivatives of 4-aminoantipyrine yield highly potent SOD mimics. The observed correlation between the SOD activity and the redox potential of the Cu^+/Cu^{2+} emphasizes the roles played by electronic as well as stereochemical factors in the biological activities of these complexes. Further work to investigate this role of copper ions by determining the lethal dose of the complex in biological systems and their pharmacological screening is in progress and will be reported in due course.

Acknowledgement

We express our sincere thanks to the Chancellor, Noorul Islam Centre for Higher Education, Kumaracoil for providing research facilities. This work was financially supported by DST, New Delhi under INSPIRE fellowship (IF 10544).

References

[1] K. E. Erkkila, D. T. Odom, J. K. Barton, *Chem. Rev.* **1999**, *99*, 2777.
[2] B. Armitage, *Chem. Rev.* **1998**, *98*, 1171.
[3] W. K. Pogozelski, T. D. Tullius, *Chem. Rev.* **1998**, *98*, 1089.
[4] H. T. Chifotides, K. R. Dunbar, *Acc. Chem. Res.* **2005**, *38*, 146.
[5] S. J. Lippard, *Chem. Rev.* **1999**, *99*, 2467.
[6] S. Yamada, *Coord. Chem. Rev.* **1999**, *192*, 537.
[7] J. R. Nitschke, *Acc. Chem. Res.* **2007**, *40*, 103.
[8] J. Lv, T. Liu, S. Cai, X. Wang, L. Liu, Y. Wang, *J. Inorg. Biochem.* **2006**, *100*, 1888.
[9] R. Gust, I. Ott, D. Posselt, K. Sommer, *J. Med. Chem.* **2004**, *47*, 5837.
[10] P. M. Selvakumar, E. Suresh, P. S. Subramanian, *Polyhedron* **2007**, *26*, 749.
[11] N. T. Madhu, P. K. Radhakrishnan, M. Grunert, *Thermochim. Acta* **2003**, *407*, 73.
[12] S. Kumar, Durga Nath Dhar and P. N. Saxena, *J. Sci. Ind. Res.* **2009**, *68*, 181.
[13] P. R. Kumar, S. Upreti, A. K. Singh, *Polyhedron* **2008**, *27*, 1610.
[14] V. Patroniak, A. R. Stefankiewicz, J.-M. Lehn, M. Kubicki, *Eur. J. Inorg. Chem.* **2005**, *10*, 4168.
[15] T. R. Li, Z. Y. Yang, B. D. Wang, D. D. Qin, *Eur. J. Med. Chem.* **2008**, *43*, 1688.
[16] C. Rice-Evans, *Curr. Med. Chem.* **2001**, *8*, 797.
[17] J. K. Swearingen, D. X. West, *Transit. Met. Chem.* **2001**, *26*, 252.
[18] J. Liu, H. Zhang, C. Chen, H. Deng, T. Lu, L. Ji, *J. Chem. Soc. Dalton Trans.* **2003**, 114.
[19] M. C. Prabahara, H. S. Bhojya Naik, *Biometals* **2008**, *21*, 675.
[20] R. N. Patel, N. Singh, K. K. Shukla, U. K. Chauhan, J. Nicols Gutierrez, A. Castineiras, *Inorg. Chim. Acta* **2004**, *357*, 2469.
[21] M. Kurtoglu, F. Purtas, S. Toroglu, *Transit. Met. Chem.* **2008**, *33*, 705.
[22] J. H. Looker, J. R. Edman and J. I. Dappen, *J. Heterocycl. Chem.* **1964**, *1*, 141.
[23] C. Adhikary, R. Bera, B. Dutta, S. Jana, G. Bocelli, A. Cantoni, S. Chaudhuri, S. Koner, *Polyhedron* **2008**, *27*, 1556.
[24] R. N. Patel, S. Kumar, K. B. Pandeya, *J. Inorg. Biochem.* **2002**, *89*, 61.
[25] C. C. Winterbourn, *Biochem. J.* **1981**, *198*, 125.
[26] W. J. Geary, *Coord. Chem. Rev.* **1971**, *7*, 81.
[27] A. D. Bansod, R. G. Mahale, and A. S. Aswar, *Russ. J. Inorg. Chem.* **2007**, *52*, 879.
[28] K. Nakamoto, *Spectroscopy and Structure of Metal Chelate Compounds*, John Wiley: New York, **1988**, p. 214.
[29] Sandipan Sarkar, Pulak K. Dhara, M. Nethaji, Pabitra Chattopadhyay, *J. Coord. Chem.* **2009**, *62*, 817.
[30] J. R. Anacona, D. Lorono, M. Azocar, R. Atencio, *J. Coord. Chem.* **2009**, *62*, 951.
[31] S. Chandra, L. K. Gupta, *Spectrochim. Acta Pt A* **2005**, *61*, 269.
[32] A. B. P. Lever, *Inorganic Electronic Spectroscopy*, 2nd edn. Elsevier: New York, **1968**.
[33] S. Chandra, L. K. Gupta, *Spectrochim. Acta Pt A* **2005**, *61*, 269.
[34] Y. Liu, Na. Wang, W. Mei, F. Chen, H. Li-Xin, L. Jian, R. Wang, *Transit. Met. Chem.* **2007**, *32*, 332.
[35] M Hamming, N Foster, *Interpretation of Mass Spectra of Organic Compounds*, Academic Press: New York, **1972**.

[36] A. S. Gaballa, M. S. Asker, A. S. Barakat, S. M. Teleb, *Spectrochim. Acta Pt A* **2007**, *67*, 114.
[37] M. Fujiwara, H. Watika, T. Matsushtla, T. Shono, *Bull. Chem. Soc. Jpn.* **1990**, *63*, 3443.
[38] K. Jeyasubramanian, S. Thambidurai, S. K. Ramalingam, R. Murugesan, *J. Inorg. Biochem.* **1998**, *72*, 101.
[39] Y. Anjaneyula, R. P. Rao, *Synth. React. Inorg. Met.-Org. Chem.* **1986**, *16*, 257.
[40] N. Dharamaraj, P. Viswanathamurthi, K. Natarajan, *Transit. Met. Chem.* **2001**, *26*, 105.
[41] J. R. Anacona, O. Nusetti, C. Gutierrez, D. Lorono, *J. Coord. Chem.* **2002**, *55*, 1433.
[42] W. G. Hanna, M. M. Moawad, *Transit. Met. Chem.* **2001**, *26*, 644.
[43] F. Saczewski, E. Dziemidowicz-Borys, P. J. Bednavski, R. Grunert, M. Gdaniec, P. Tabin, *J. Inorg. Biochem.* **2006**, *100*, 1389.
[44] A. K. Das (Ed.), *Medicinal Aspects of Bioinorganic Chemistry*, CBS: Shahdara, Delhi, **1990**, chap. 3.
[45] A. M. Díaz, R. Villalonga, R. Cao, *J. Coord. Chem.* **2009**, *62*, 100.
[46] M. Karatepe, F. Karatas, *Cell Biochem. Funct.* **2005**, *24*, 547.
[47] K. H. Kumar, P. T. Perumal, *Tetrahedron* **2007**, *63*(38), 9531.
[48] M. J. Waring, in *Drug Action at the Molecular Level* (Ed.: G. C. K. Roberts), Macmillan: London, **1977**, p. 167.
[49] S. Dhar, P. A. N. Reddy, M. Nethaji, S. Mahadevan, M. K. Saha, A. R. Chakravarty, *Inorg. Chem.* **2002**, *41*, 3469.
[50] Q. S. Li, P. Yang, H. F. Wang, M. L. Guo, *J. Inorg. Biochem.* **1996**, *64*, 181.
[51] S. Belaid, A. Landreau, S. Djebbar, O. Benali-Baitich, G. Bouet, J. P. Bouchara, *J. Inorg. Biochem.* **2008**, *102*, 63.
[52] M. S. Surendra Babu, K. Hussain Reddy, Pitchika G. Krishna, *Polyhedron* **2007**, *26*, 572.
[53] F. H. Li, G. H. Zhao, H. X. Wu, H. Lin, X. X. Wu, S. R. Zhu, H. K. Lin, *J. Inorg. Biochem.* **2006**, *100*, 36.
[54] S. Shi, J. Liu, J. Li, K. C. Zheng, X. M. Huang, C. P. Tan, L. M. Chen, L. N. Ji, *J. Inorg. Biochem.* **2006**, *100*, 385.

